

# Coronal Hole Analysis and Prediction using Computer Vision and LSTM Neural Network

Juyoung Yun

State University of New York Korea, Data and Intelligent Computing Laboratory, Republic of Korea

Stony Brook University, Department of Computer Science, USA

January 17, 2023

juyoung.yun@stonybrook.edu

## Abstract

As humanity has begun to explore space, the significance of space weather has become apparent. It has been established that coronal holes, a type of space weather phenomenon, can impact the operation of aircraft and satellites. The coronal hole is an area on the sun characterized by open magnetic field lines and relatively low temperatures, which result in the emission of the solar wind at higher than average rates. In this study, To prepare for the impact of coronal holes on the Earth, we use computer vision to detect the coronal hole region and calculate its size based on images from the Solar Dynamics Observatory (SDO). We then implement deep learning techniques, specifically the Long Short-Term Memory (LSTM) method, to analyze trends in the coronal hole area data and predict its size for different sun regions over 7 days. By analyzing time series data on the coronal hole area, this study aims to identify patterns and trends in coronal hole behavior and understand how they may impact space weather events. This research represents an important step towards improving our ability to predict and prepare for space weather events that can affect Earth and technological systems.

## 1 Introduction

Space weather refers to a variety of phenomena that occur in the vast expanse of space between the Sun and the Earth, caused by solar activity and impacting the Earth's environment [Davis, 1990, Sandford, 1999] including the sun and the solar wind, as well as the Earth's magnetosphere, ionosphere, and thermosphere [NOAA, n.d.]. These conditions can have a variety of impacts on Earth, including disruptions to satellite and aircraft operations, as well as impacts on power grids and GPS navigation [Filjar, 2006, Rama Rao et al., 2009]. Space weather is influenced by a variety of factors, including solar activity, such as solar flares and coronal mass ejections [Schwenn, 2006]. For example, geomagnetic storms caused by space weather can disrupt satellite communications, leading to disruptions in phone and internet services [Rama Rao et al., 2009]. These storms

can also affect the accuracy of GPS signals, which are used for navigation and positioning by a wide range of technologies, including aircraft, vehicles, and smartphones [Filjar, 2006, Rama Rao et al., 2009]. Space weather can also have impacts on power grids, as geomagnetic storms can induce currents in power lines, leading to voltage fluctuations and even power outages [Boteler, 2013, Kappenman, 1996]. In addition, space weather can affect the Earth's ionosphere, which is the region of the Earth's atmosphere that is ionized by solar radiation and is responsible for reflecting radio waves [NOAA, n.d.]. This can lead to disruptions in radio communications, including shortwave radio and high-frequency (HF) radio [NOAA, n.d.]. Given the potential impacts of space weather on our daily lives and infrastructure, it is important to study and understand space weather in order to better predict and mitigate its effects.

A coronal hole is a region on the sun's surface where the solar corona, or outer atmosphere, is relatively cool and has a lower density than the surrounding areas. Coronal holes are characterized by the absence of strong magnetic fields, which typically trap and heat the solar plasma, and are often observed as dark areas in images of the sun's corona [Cranmer, 2009]. Coronal holes are thought to be the source of high-speed solar wind streams, which are streams of ionized gas that flow outward from the sun at speeds of up to 800 km/s [Cranmer, 2009]. These high-speed solar wind streams can cause geomagnetic storms when they interact with the Earth's magnetosphere, leading to disruptions in satellite and aircraft operations, as well as impacts on power grids and GPS navigation [Filjar, 2006, Rama Rao et al., 2009]. Space weather events, such as geomagnetic storms caused by coronal holes, can have significant impacts on aviation operations. These events can disrupt satellite communications and GPS signals, leading to disruptions in airline operations and increased workload for air traffic controllers. In the context of military aircraft operations, these disruptions can pose significant risks and potentially have fatal consequences. Therefore, it is important to develop strategies for predicting and preparing for these events in order to mitigate their potential impact on aircraft missions and operations.

In this study, we developed a Computer Vision model

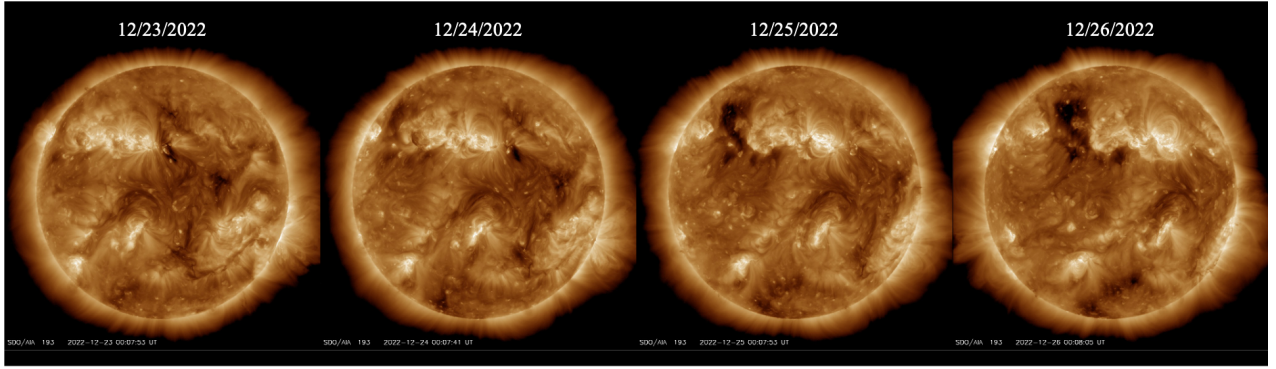


**Figure 1.** A visual representation of the changes in coronal hole size and position over a 4-day period from December 23, 2022 to December 26, 2022, as captured by the NASA Heliophysics Integrated Observatory Network. The image illustrates the dynamic nature of coronal holes and their potential impact on space weather events.

that uses a non-learning approach to automatically identify the coronal hole area of the sun. By applying this model we collect daily dataset of 10 years worth of coronal hole area data, we are able to quickly train a deep learning model to predict the coronal hole area in a specific area in the future. Our approach represents a novel application of Computer Vision and deep learning techniques for coronal hole detection. By using these techniques, we were able to quickly and accurately forecast the size of coronal holes. This study demonstrates the potential of using Computer Vision and deep learning approaches to enhance our understanding of space weather and improve our ability to predict its impacts on Earth. In addition, this study aims to contribute to this goal by identifying methods for predicting the location of coronal holes in advance, in order to anticipate and prepare for potential geomagnetic storms that could affect aviation operations. By improving our ability to forecast the location of coronal holes, we can help to reduce the potential impacts of space weather events on aviation operations and enhance the safety of aircraft missions.

## 2 Background

### 2.1 Observation of Coronal Hole

One method for observing coronal holes involves observations of the sun in extreme ultraviolet (EUV) wavelengths, which are typically emitted by hot, low-density plasma in the corona [Lemen et al., 2012]. EUV observations can be made using telescopes on spacecraft, such as the Solar Dynamics Observatory (SDO), which has a EUV telescope called the Atmospheric Imaging Assembly (AIA) [Lemen et al., 2012]. AIA 193 is a telescope on the Solar Dynamics Observatory (SDO) satellite, which is a spacecraft launched by NASA in 2010 to study the sun and its influence on Earth and the solar system [NASA, n.d.]. The AIA 193 telescope is designed to observe the sun in the extreme ultraviolet (EUV) wavelength range, which is important for studying the sun's atmosphere and the dynamics of solar eruptions, such as solar flares and coronal mass ejections [NASA, n.d.]. The AIA 193 channel (Fig. 1) is one of several channels on the AIA instrument that is used to observe the sun's atmosphere at a specific wavelength of 193

angstroms, which corresponds to a temperature of about 1.5 million degrees Celsius [Lemen et al., 2012]. See Fig. 1 for images of the coronal holes for 4 days. Another method for detecting coronal holes involves using computational models to simulate the sun's magnetic field and plasma behavior. These models can be based on various mathematical techniques, such as magnetohydrodynamic (MHD) models or potential field source surface (PFSS) models [Inoue, 2016]. These models can be used to predict the location and size of coronal holes based on the observed properties of the sun's magnetic field and the known physical laws governing the behavior of plasma in the solar atmosphere [Inoue, 2016].

### 2.2 Coronal Mass Ejection

A coronal mass ejection (CME) is a massive burst of solar plasma and magnetic field that is ejected from the Sun's corona into interplanetary space [Webb & Howard, 2012, Yashiro et al., 2004]. CMEs are typically associated with solar flares and other forms of solar activity and are thought to be driven by the explosive release of energy stored in the Sun's magnetic field [Webb & Howard, 2012, Yashiro et al., 2004]. CMEs can vary in size and intensity and can contain billions of tons of solar plasma and magnetic field [Webb & Howard, 2012, Yashiro et al., 2004]. When a CME is directed towards Earth, it can take one to four days to reach our planet, depending on the speed of the CME and the distance between the Sun and Earth [Webb & Howard, 2012, Yashiro et al., 2004]. CMEs can have a significant impact on Earth's space environment and technological systems. When a CME reaches Earth, it can interact with the Earth's magnetic field and produce geomagnetic storms, which can affect the Earth's ionosphere and magnetosphere and lead to changes in the Earth's geomagnetic field and the flow of charged particles within these regions [Schwenn, 2006].

### 2.3 Corotating Interaction Regions

Corotating interaction regions (CIRs) are dynamic features in the solar wind characterized by rapid changes in the plasma and magnetic field over a relatively short distance [Heber, Sanderson, & Zhang, 1999]. These regions are formed by the interaction between high-speed and low-

speed solar wind streams and are often associated with coronal holes [Heber, Sanderson, & Zhang, 1999]. When a CIR reaches Earth, it can interact with the Earth’s magnetic field and produce geomagnetic storms, which can have a range of impacts on the Earth’s space environment and technological systems, including the ionosphere and magnetosphere, as well as changes in the Earth’s geomagnetic field and the flow of charged particles within these regions [Schwenn, 2006]. Understanding the formation and evolution of CIRs is important for predicting and mitigating their potential impacts on Earth.

The frequency of CMEs is highest during solar maximum periods [Webb & Howard, 2012, Yashiro et al., 2004], which means that storms during these periods are typically caused by CMEs [Richardson et al., 2001]. The frequency of well-formed Corotating Interaction Regions (CIRs) with 27-day recurrences peaks during the later stages of the solar cycle [Mursula & Zeiger, 1996], making storms in the declining phase more likely to be CIR-driven [Richardson et al., 2001]. It’s worth noting that Interaction Regions (IRs) produced by non-recurring high-speed streams can occur throughout the solar cycle [Bobrov, 1983] and can cause non-recurring geomagnetic activity throughout the solar cycle [Richardson et al., 2000], although the geomagnetic events they cause are generally weaker than the recurring events of the declining phase [Bobrov, 1983].

## 2.4 Geomagnetic Storm

A geomagnetic storm is a disturbance of the Earth’s magnetosphere caused by high-speed solar wind streams emanating from coronal holes on the sun’s surface [Eoin et al., 2003]. These storms can cause variations in the Earth’s magnetic field, which can affect the accuracy of navigation systems that rely on the magnetic field, such as those used by some aircraft [Filjar, 2006]. Geomagnetic storms can also disrupt satellite communications [Rama Rao et al., 2009] and affect the accuracy of global positioning system (GPS) signals [Filjar, 2006, Rama Rao et al., 2009]. The intensity of a geomagnetic storm is commonly measured using the Kp index, which is a global measure of geomagnetic activity that ranges from 0 (no geomagnetic activity) to 9 (severe geomagnetic storm) [NASA, n.d.]. Geomagnetic storms with a Kp index of 5 or higher are considered significant and can have significant impacts on satellite and aircraft operations [Rama Rao et al., 2009]. They can also cause auroras, or Northern and Southern Lights, which are colorful displays of light in the Earth’s atmosphere visible at high latitudes [Rama Rao et al., 2009]. Geomagnetic storms can have a range of impacts on aircraft operations, including disruptions to navigation systems, satellite communications, and power systems. The impact of solar events, such as coronal mass ejections (CMEs) and solar flares, on the Earth can be measured using various geomagnetic indices, such as the auroral electrojet (AE) index, disturbance storm time (Dst) index, ASY/SYM index, and Kp and ap/Ap indices, among others, as indicators [Badruddin & Falak, 2016].

## 2.5 Coronal Hole and AP

The standardized Ks and planetary Kp indices, which are used to measure geomagnetic activity, were first introduced by Bartels [1949]. These indices are calculated from observatory-specific K indices that are recorded every three hours [Bartels, 1938]. The daily Ap index is derived from KP. AP index, or planetary magnetic activity index, is a measure of the intensity of geomagnetic activity on Earth [Rama Rao et al., 2009]. Geomagnetic activity is caused by the interaction between Earth’s magnetosphere and the solar wind, which is a stream of charged particles that are emitted by the Sun. When the solar wind is stronger and more variable, it can interact more strongly with Earth’s magnetosphere, resulting in increased geomagnetic activity [Eoin et al., 2003]. Strong CIRs and the faster CH HSS can impact Earth’s magnetosphere enough to cause periods of geomagnetic storming to the G1-G2 (Minor to Moderate) levels, although rarer cases of stronger storming may also occur. Geomagnetic storms are classified using a five-level NOAA Space Weather Scale. The larger and more expansive coronal holes can often be a source for high solar wind speeds that buffet Earth for many days [Cranmer, 2009]. The AP index is a measure of geomagnetic activity, which is the response of Earth’s magnetosphere to solar wind and other solar activity. The AP index is one of several indices that are used to quantify geomagnetic activity and assess the potential impacts of space weather events on Earth. It is based on the number of auroral oval boundary crossings observed at a number of observatories around the world [NOAA, 2021].

## 3 Method

In this work, we first developed a computer vision model that detects the area of the coronal hole to predict the area of the coronal hole. This is a different technique from learning the coronal hole image itself, and learning the coronal hole image itself requires frequent training due to the characteristic of time series data, and image learning consumes much more time and computing resources than numerical learning. This is unsuitable for irregularly changing weather models and prevents rapid prediction and contrast. Therefore, we use a technique that quickly identifies and quantifies only the coronal hole region, rather than training the image, and then quickly learns and predicts the numerical data by deep learning techniques. This is to help forecasters quickly identify and predict changing coronal hole areas to prepare for situations that will occur. In Fig. 2, we detect and extract coronal holes by using computer vision techniques and finally predict the future trend of the coronal hole through deep learning.

### 3.1 Coronal Hole Detection

Identification of the Coronal hole region is traditionally confirmed through the naked eye of the image data. There is a disadvantage in that when CH is detected through the naked eye, different results can be obtained for each person. Currently, an automatic system has been developed for objective results [Heinemann et al., 2019]. In addition, a

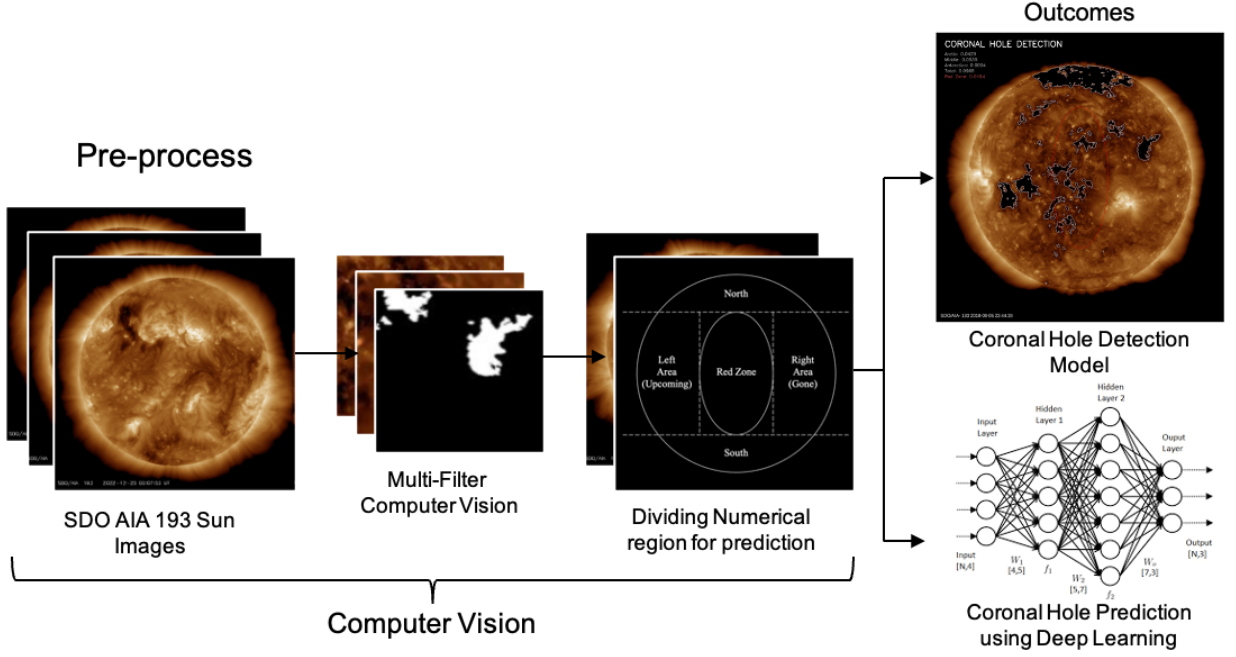


**Figure 2.** A depiction of the regions used to calculate the area of the coronal hole in the sun, as defined by the binary based Coronal Hole Detection model (BCH). The original AIA image is captured by the NASA Heliophysics Integrated Observatory Network and illustrates the Arctic, Antarctic, Middle, Red Zone, and Total regions used to calculate coronal hole area.

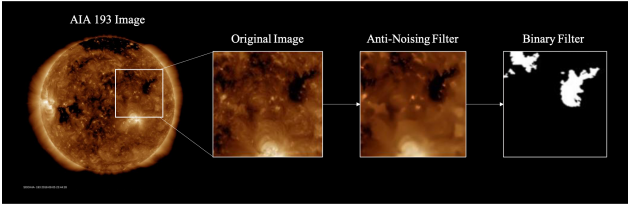


**Figure 3.** A depiction of the multi-filters computer vision based coronal hole detection techniques applied to an original AIA 193 image captured by the NASA Heliophysics Integrated Observatory Network. The image illustrates the use of various filters such as anti-noising and binary filters to accurately identify and measure the area of coronal holes in the sun.

model for detecting CH area through a CNN deep learning model has been developed [Jarolim, 2021]. In the case of a deep learning-based CH detection model, there is a disadvantage that image data must be learned. We create a simple computer vision model that detects coronal Holes and computes the area without image learning, and develop a time series prediction deep learning model based on its numerical data. For detecting the coronal hole, we just multi-filter detection model (Fig. 3). We use AIA193 images for detecting the coronal holes in the sun. First of all, to clearly identify the coronal hole region in the image, we use anti-noising techniques. The anti-noising method is used to reduce the presence of ambiguous and noisy areas in AIA 193 images, making black areas more visible. While it is not possible to completely eliminate noise, reducing its visibility can be achieved through the use of techniques such as the non-local means anti-noising (NLmeans) tech-

nique [Buades, 2005]. This technique compares the similarity between patches containing pixels to be modified and patches containing each pixel in the middle. The pixel values of patches with a high level of similarity are given a larger weight, and the resulting value is added to the current pixel value. By implementing the Noise Reduction with NLmeans technique built into the OpenCV library, it is possible to significantly reduce the noise in an image, making features such as coronal holes more prominent.

The anti-noising process can be represented as taking an input image  $I$  and producing a anti-noised output image  $J$ .

$$J(x) = \frac{1}{W(x)} \cdot \sum(I(y) \cdot K(x, y))$$

Where  $x$  and  $y$  are pixel positions,  $W(x)$  is a normalization term, and  $K(x, y)$  is a weighting function that measures the similarity between pixels  $x$  and  $y$ . The weighting function  $K(x, y)$  is typically defined as:

$$K(x, y) = \exp\left(-\frac{\|I(x) - I(y)\|^2}{h^2}\right)$$

Where  $\|I(x) - I(y)\|^2$  is the squared Euclidean distance between the pixel values at positions  $x$  and  $y$ , and  $h$  is a parameter known as the "smoothing parameter" that controls the strength of the anti-noising. We used Image Binarization technique to change the coronal hole to white and the rest of the region to black to identify only the coronal hole region in the solar image. Image Binarization is the process of converting a gray-scale or color image into a binary image, which is an image consisting only of black and white pixels [Gonzalez & Woods, 2006]. One method for achieving this is the threshold method, which involves setting a threshold value and converting all pixels with a value above the threshold to white, and all pixels with a value below

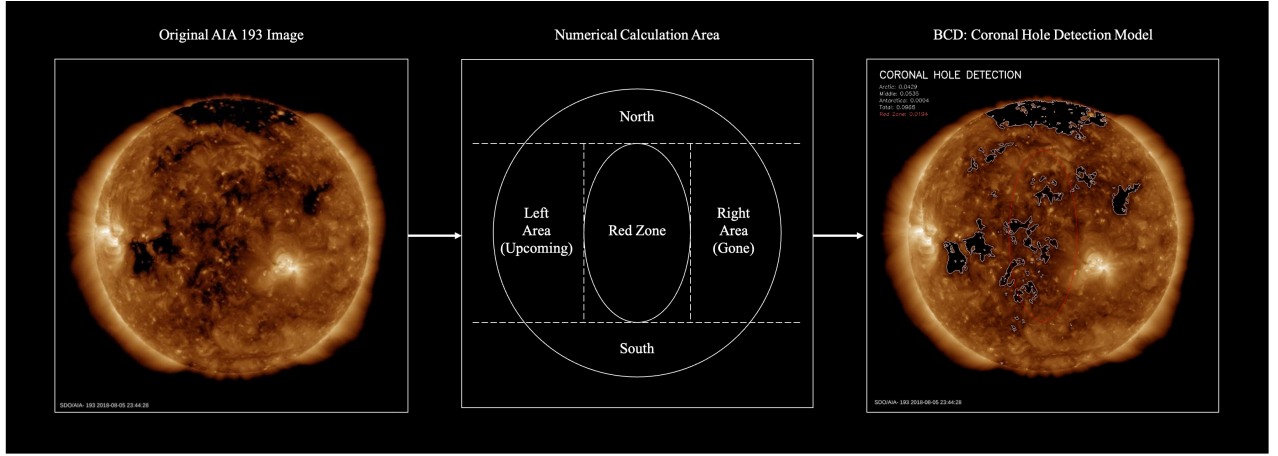


**Figure 4.** Calculation Regions of Coronal Hole (Original AIA 193 image courtesy The NASA Heliophysics Integrated Observatory Network)

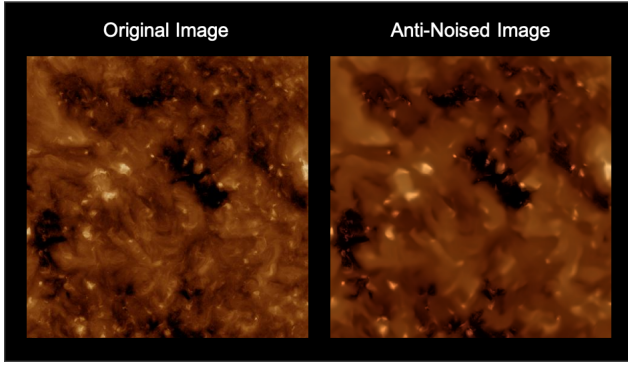


**Figure 5.** Original Image and Anti-noised Image (Original AIA 193 image courtesy The NASA Heliophysics Integrated Observatory Network)

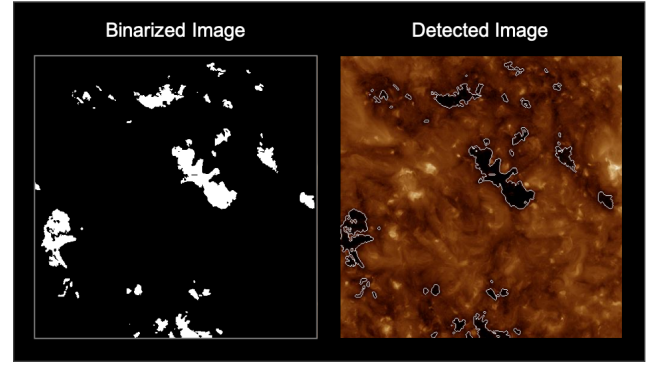


**Figure 7.** Binarized Image and Contoured Image (Original AIA 193 image courtesy The NASA Heliophysics Integrated Observatory Network)

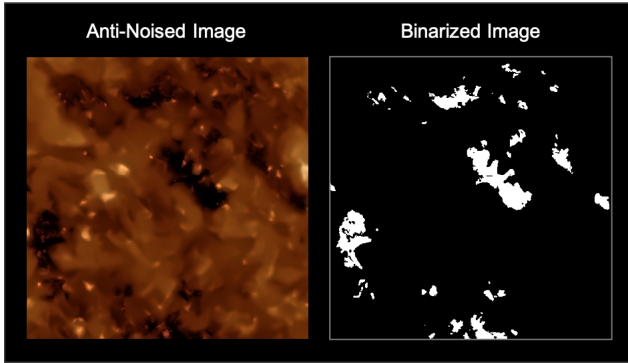


**Figure 6.** Anti-noised Image and Binarized Image (Original AIA 193 image courtesy The NASA Heliophysics Integrated Observatory Network)

the threshold to black [Gonzalez & Woods, 2006]. Image binarization can be used to divide an image into important and non-critical areas and is commonly used for tasks such as object recognition, character recognition, and fingerprint recognition. In this case, image binarization is used to binarize the AIA 193 image that has undergone noise reduction in order to speed up the process of coronal hole recognition

and calculation. The process of image binarization involves converting an image with values ranging from 0 to 255, with each pixel represented by 8 bits, to an image with values of 0 or 1 based on a given threshold. Pixels with values above the threshold are assigned a value of 1, while pixels with values below the threshold are assigned a value of 0. The method of binarizing an RGB image first converts the average value of RGB into a black-and-white image with a value of 0 to 255 per pixel, and then converts the pixel value to 0 and 255 based on the threshold. In the case of RGB888, which is 24 bits per pixel, the pixel values of the black-and-white image are as follows [Gonzalez & Woods, 2006]:

$$X = (X_r + X_g + X_b)/3$$

After calculating as above, values less than or equal to 100 based on the threshold value 100 are converted to 0, and values greater than 100 are converted to 255. Image binarization allows us to identify the coronal hole region. This method binarized the image and detected that only the coronal hole region appeared white in the AIA 193 image. Based on this Binary Image, we find the Image Contour of Coronal Hole and display it in the original AIA 193 image. For contouring the coronal hole we used the Laplacian of Gaussian (LoG) operator [Gonzalez & Woods, 2006].

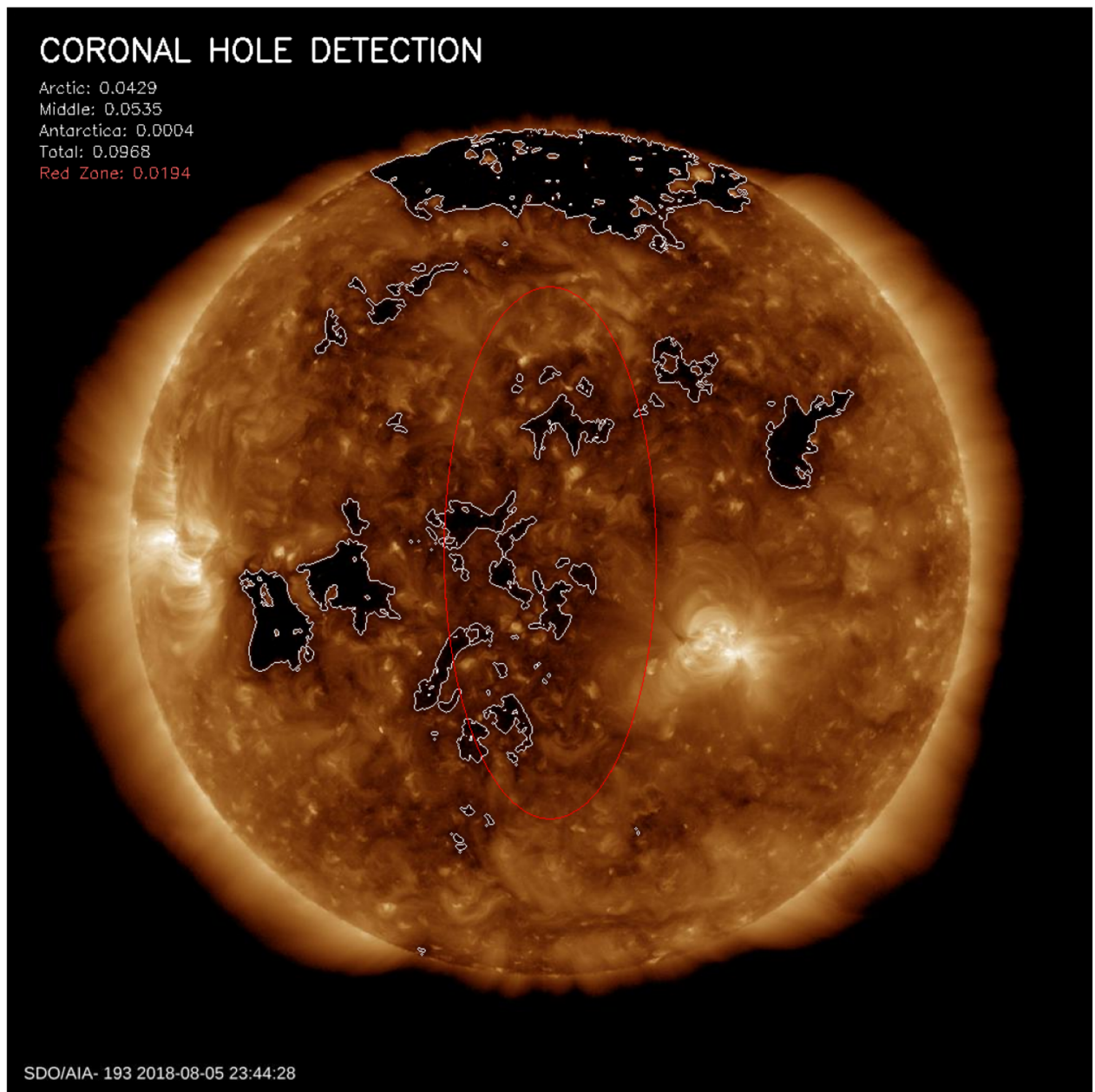


**Figure 8.** Coronal Hole Detection Model based on Multi-filter Computer Vision Techniques (Original AIA 193 image courtesy The NASA Heliophysics Integrated Observatory Network)

This algorithm typically works by detecting changes in the intensity or color of the pixels in the image, and marking those pixels as edges [Gonzalez & Woods, 2006]. The Laplacian of Gaussian (LoG) operator [Marr, 1980] is a kernel that is used for edge detection in images. It is constructed by taking the second derivative of a Gaussian function. The mathematical formula for the Laplacian of Gaussian operator:

$$L(x, y) = (x^2 + y^2 - \sigma^2) \cdot \frac{G(x, y)}{(2\pi\sigma^4)}$$

Where  $x$  and  $y$  are the pixel positions, sigma is a parameter that controls the width of the Gaussian function, and  $G(x, y)$  is the Gaussian function:

$$G(x, y) = \frac{1}{(2\pi\sigma^2)} \cdot \exp\left(\frac{-(x^2+y^2)}{(2\cdot\sigma^2)}\right)$$

The Laplacian of Gaussian is used for edge detection because it is sensitive to abrupt changes in image intensity, which often correspond to object boundaries in images.

Contouring was used to allow users to easily check the area of the coronal hole. Looking at the Binary Based Coronal Hole Detection(BCH) model in Fig. ??, it is easy to check the coronal hole area.

To calculate the area of the region, we calculated the area of the specific region as a ratio of the area of the sun's plane (Fig. 4). The solar equator is a strong area that affects the Earth. It is generally believed that coronal holes located near the solar equator are more likely to result in a co-rotating interaction region (CIR) passage and higher solar wind speeds at Earth, which can impact the Earth's magnetosphere and potentially cause geomagnetic storms [NOAA,

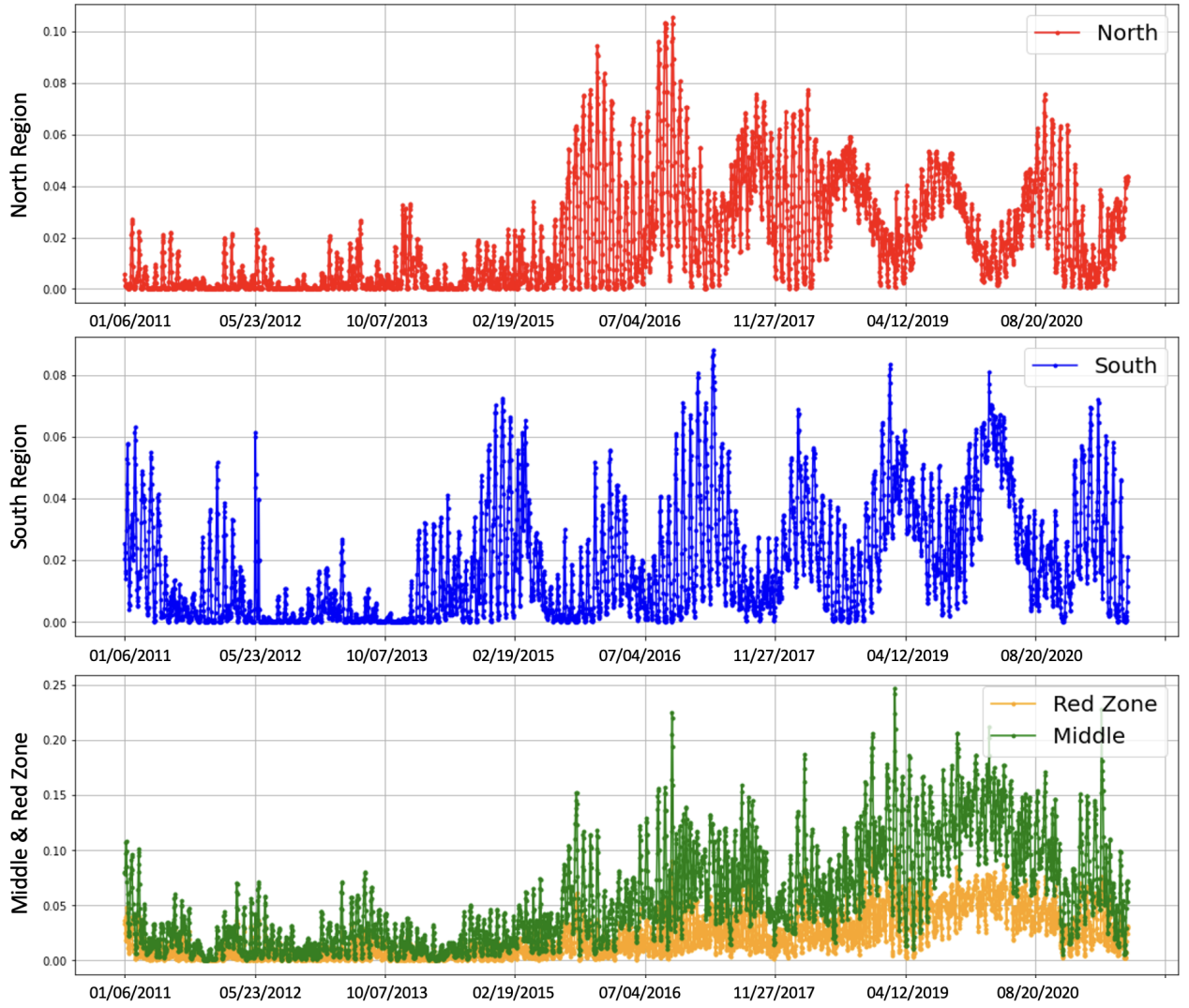


**Figure 9.** Daily Coronal Hole Data for each region of the sun, calculated over a period of 3857 days from January 6, 2011 to August 10, 2021, obtained by the binary-based Coronal Hole Detection model (BCH). The graph presents the variation of coronal hole area for each regions of the sun over time.

2021]. Coronal holes are most commonly observed at high latitudes near the Sun’s poles, but they can also occur at lower latitudes and be isolated from the polar holes. Persistent coronal holes are long-lasting sources of high-speed solar wind streams that can affect Earth. When a high-speed stream from a coronal hole interacts with the slower ambient solar wind, it can create a compression region called a co-rotating interaction region (CIR). From the perspective of a fixed observer in interplanetary space, the CIR will appear to lead the coronal hole high-speed stream. Geomagnetic storms are classified using a five-level NOAA Space Weather Scale, with levels ranging from G1 (minor) to G5 (extreme) [NOAA, 2021].

In order to analyze the coronal hole area on the sun, a technique known as Image Binarization was employed. This method involves converting AIA193 images into binary form, where the coronal hole area is revealed as white pixels. By drawing Image Contours on the AIA 193 images, we were able to confirm that the coronal hole area was accurately detected, as shown in Fig. ???. This tech-

nique allows for the extraction of a total of five data points for the Arctic(North), Antarctic(South), Middle, Red Zone, and the entire region(Total) from a single image. To conduct this study, we collected a total of 3857 daily coronal hole area data points from 01/06/2011 to 08/10/2021 using AIA 193 image data from NASA’s Solar Dynamics Observatory (SDO). The images were taken at around 0:00 UTC every day, which allowed for the collection of daily data points. Using these data points, we were able to make predictions about the area of the coronal hole in the equatorial region of the Sun, which has the highest probability of producing Coronal Mass Ejections (CMEs) and Corotating Interaction Regions (CIRs). In our model, we refer to these regions as the Red Zone and Middle.

## 3.2 Data Analysis

### 3.2.1 Analysis Summary

Fig. 9 illustrates the results of a study that analyzed the area of the solar corona hole on August 10, 2021, and compared

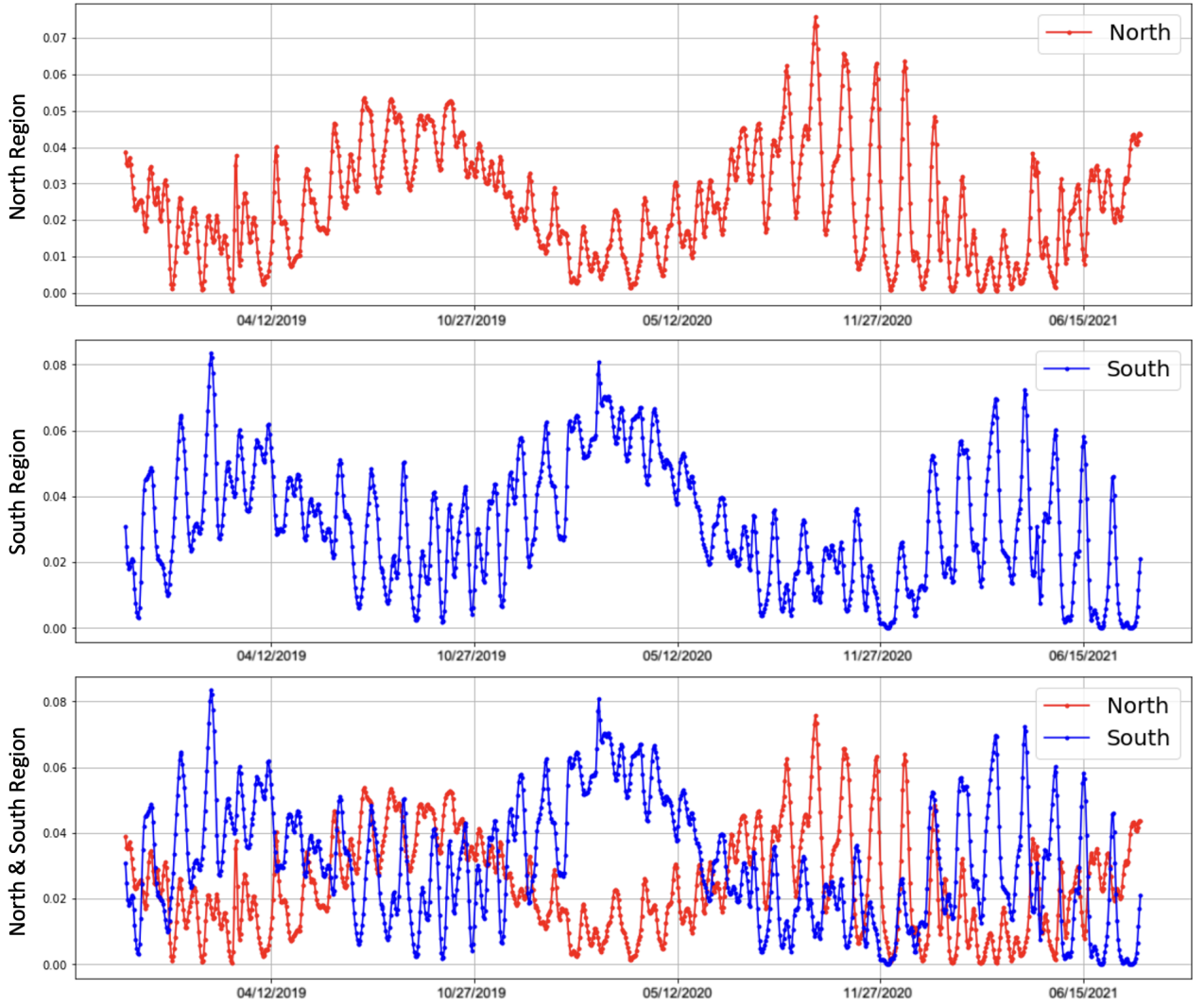


**Figure 10.** A comparison of daily coronal hole data for the south and north regions of the sun over a 1000-day period from November 13, 2018 to August 10, 2021 as obtained by the binary-based Coronal Hole Detection model (BCH). The graph illustrates the variation of coronal hole area in the south and north regions over time, and the consistency of the polarity rule.

it to data from Jan 6, 2011. The analysis revealed that the overall coronal hole area has gradually increased over the past 10 years. In particular, the area of the middle region has increased significantly, suggesting that the coronal hole is expanding. However, it is important to note that 10 years of data is a relatively short time frame for analyzing solar trends, and more long-term data is needed to fully understand the dynamics of the corona hole.

Solar scientists have been studying the solar corona for many decades, and it is known that the corona is highly dynamic and subject to frequent changes. The expansion of coronal holes has been observed to be correlated with the solar cycle, an approximately 11-year cycle of solar activity that is characterized by the appearance and disappearance of sunspots, flares, and coronal mass ejections. It is possible that the expansion of the coronal hole observed in the present study is related to the current phase of the solar cycle. However, more research is needed to establish a causal relationship between the solar cycle and the expansion of coronal holes. This analysis presented in Fig. 9 provides evidence that the overall coronal hole area has gradually in-

creased over the past 10 years, with the middle area showing a significant increase. While this trend suggests that the coronal hole is expanding, it is important to note that more long-term data is needed to fully understand the dynamics of the corona hole and its relationship with the solar cycle. Further research is needed to gain insights into the underlying physical processes that drive the expansion of coronal holes, and to develop predictive models of solar activity that can help to forecast space weather events that can impact satellite and power grids operations on Earth.

### 3.2.2 Pole Region Analysis

Fig. 10 illustrates the results of our analysis of the area of the coronal hole over a period of 1000 days using our detection model. As shown in the figure, it is evident that the area of the coronal hole in the north pole region and the south pole region of the Sun is generally opposite to each other [Abramenko & Biktimirova, 2022]. This phenomena, known as the "polarity rule," is consistent with the understanding that the coronal holes that occur near the north and

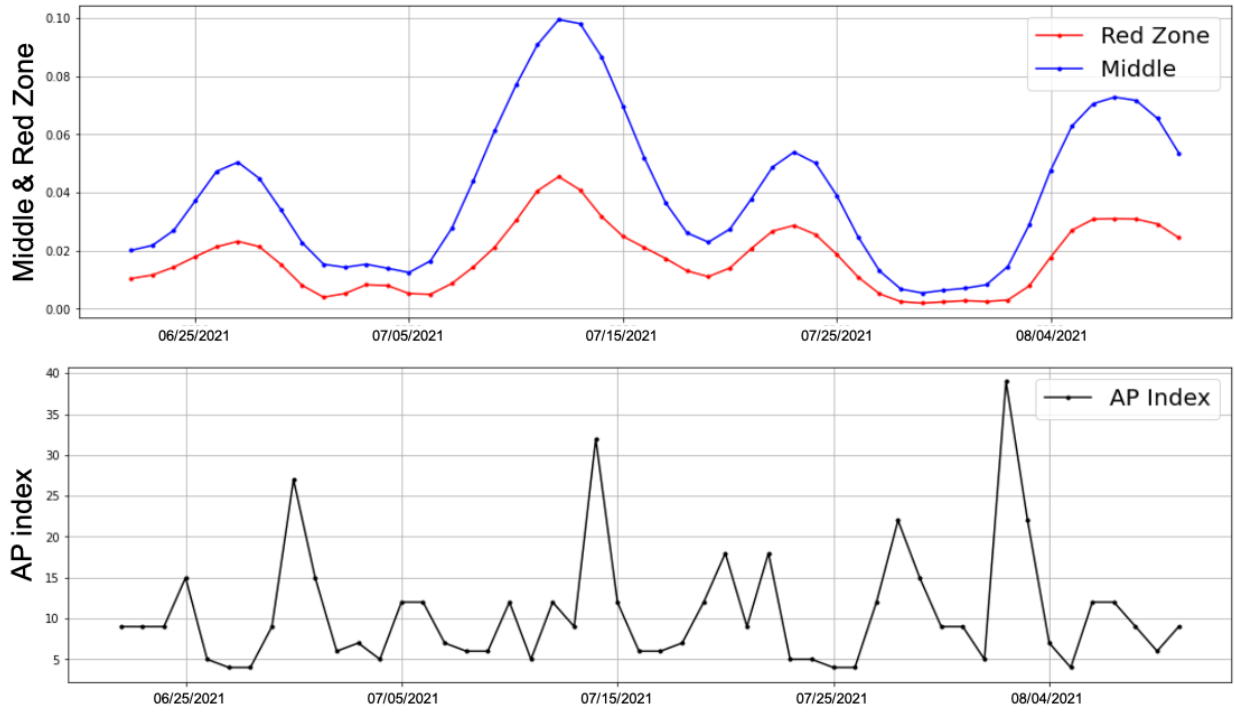


**Figure 11.** The AP index and the data calculated for the middle and redzone regions of coronal hole on the sun for a period of 50 days from June 22, 2021 to August 10, 2021, as obtained by the binary-based Coronal Hole Detection model (BCH). The graph illustrates the correlation between the AP index and the coronal hole area in the middle and redzone regions of the sun. (AP index data courtesy of World Data Center for Geomagnetism, Kyoto)

south poles of the Sun are often opposite to each other in terms of their magnetic field configuration and the direction of the solar wind stream that they produce [McIntosh, 1991]. The location of a coronal hole on the Sun can affect the intensity and duration of the solar wind stream that it produces, as well as the direction in which the stream travels [Cranmer, 2009]. When a coronal hole is located near the north pole of the Sun, the solar wind stream it produces may be directed towards the south, and vice versa for a coronal hole located near the south pole [Abramenko & Biktimirova, 2022, Cranmer, 2009]. This is because the orientation of the Sun’s magnetic field causes the solar wind particles to be deflected in opposite directions at the north and south poles [Abramenko & Biktimirova, 2022, Cranmer, 2009].

Our results provide further evidence supporting the claims of previous studies that have studied the polarities of coronal holes and their relationship with the solar wind stream. This study adds to the current understanding of the dynamics of coronal holes by providing a large dataset of coronal hole areas over a 1000-day period and by demonstrating the consistency of the polarity rule. However, it is important to note that this study only covers a 1000-day period which is relatively short and more long-term data is needed to fully understand the dynamics of the coronal hole and its relationship with the solar cycle.

### 3.2.3 Middle Region Analysis

Accurate prediction of the area of coronal holes located at or near the solar equator is crucial for anticipating potential geomagnetic disturbances on Earth. These disturbances, as measured by the AP index, can be caused by the high-speed solar wind streams produced by coronal holes, which can interact with Earth’s magnetosphere and cause geomagnetic storming. Geomagnetic storms can have a wide range of impacts on human activities, including power grid failures, communication and navigation disruptions, and damage to satellites. Thus, it is important to develop effective tools for forecasting geomagnetic activity and mitigating its impacts. Our study aimed to investigate the relationship between the size of the coronal hole in the Middle region and the intensity of geomagnetic activity on Earth. To this end, we developed a BCH (coronal hole area) model that allows for the accurate measurement of coronal hole areas. By using this model, we were able to confirm that there is a strong correlation between the size of the coronal hole in the Middle region and the intensity of geomagnetic activity on Earth. Specifically, we found that when the coronal hole in the Middle region reaches a local maximum in size, there is a corresponding increase in the AP value after 3-4 days. This suggests that the BCH model can be an effective tool for forecasting geomagnetic activity and helping to mitigate the potential impacts of these disturbances. It is worth noting that the BCH model is based on the AIA 193 images from NASA’s Solar Dynamics Observatory, which provides daily images of the solar corona. This data is essential for

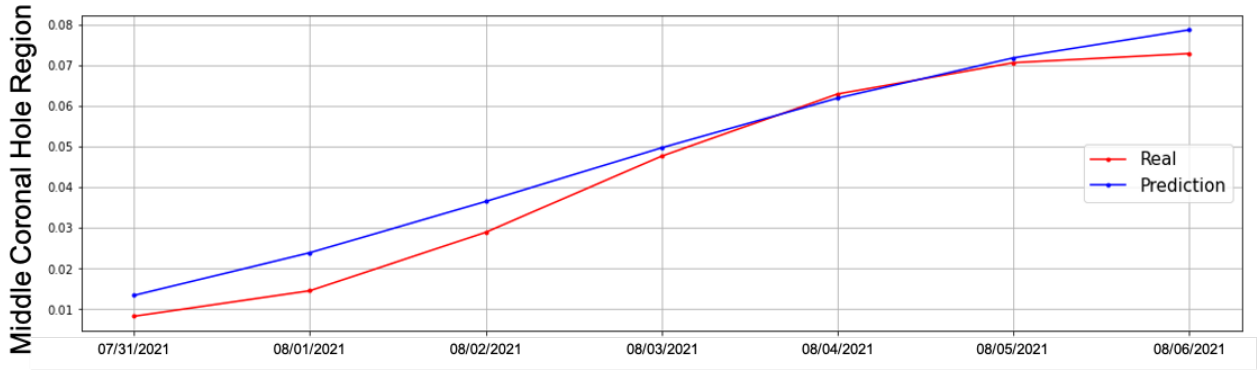


**Figure 12.** A comparison of actual middle area and predicted values for a 7-day period from July 31, 2021 to August 06, 2021, obtained after training the area data of 3847 middle coronal hole using LSTM from January 06, 2011 to July 30, 2021. The graph illustrates the accuracy of the LSTM model in predicting the area of the coronal hole in the middle region over a short-term period.

detecting coronal holes and measuring their area.

If the area of the red zone and middle area increases rapidly, it is likely that the AP index will also rise after a few days. This relationship can be observed in the graph shown in Fig. 11. The rapid increase in the area of the Red Zone and Middle area is likely caused by solar activity, such as solar flares or coronal mass ejections, which can disrupt the Earth's magnetosphere. It is important to monitor the area of the Red Zone and Middle area, as well as other indicators of solar activity, in order to anticipate and prepare for potential increases in the AP.

These increases in the AP can have a range of impacts, including disruptions to satellite and radio communications, as well as increased radiation risks for astronauts and aircraft crews. Geomagnetic activity is caused by the interaction between Earth's magnetosphere and the solar wind, which is a stream of charged particles that is emitted by the Sun [Eoin et al., 2003]. When the solar wind is stronger and more variable, it can interact more strongly with Earth's magnetosphere, resulting in increased geomagnetic activity [Eoin et al., 2003]. The larger and more expansive coronal holes can often be a source for high solar wind speeds that buffet Earth for many days [Cranmer, 2009]. This suggests that it is important for us to detect and predict coronal holes in the middle regions.

### 3.3 Prediction

#### 3.3.1 Recurrent Neural Network

A recurrent neural network (RNN) is a type of artificial neural network that is designed to process sequential data. It is called "recurrent" because it performs the same task for every element of a sequence, with the output being dependent on the previous calculations. This allows the network to retain information from the past and use it to inform the current output. One of the key features of RNNs is the use of hidden state vectors, which allow the network to capture and retain long-term dependencies in sequential data. This is in contrast to traditional feedforward neural networks, which do not have the ability to retain information from previous input elements.

However, There are several weaknesses of using recurrent neural networks (RNNs) for time-series forecasting. First of all, RNNs have limited memory and are not able to store long-term dependencies in the data effectively. This can be a problem for time series that have complex long-term dependencies, as the network may not be able to capture and utilize these dependencies to make accurate forecasts [Bengio, 1994]. In addition, RNNs can suffer from the vanishing gradient problem, where the gradients of the parameters with respect to the loss function become very small during training [Bengio, 1994]. This can make it difficult for the network to learn and make accurate predictions. RNNs can also suffer from the exploding gradient problem, where the gradients become too large and cause the network to diverge [Pascanu, Mikolov, & Bengio, 2013].

#### 3.3.2 Long Short Term Memory

Long Short-Term Memory (LSTM) is a type of recurrent neural network (RNN) that is able to remember past input sequences and use them to inform the processing of future input. It is often used in natural language processing and speech recognition tasks because it is able to handle variable-length input sequences and retain information over long periods of time. The LSTM architecture was introduced by Hochreiter & Schmidhuber [1997]. There are some advantages of using Long Short-Term Memory (LSTM) networks. First of all, LSTM has an ability to remember past input for long periods of time since LSTM networks are able to retain information over many time steps, making them well-suited for tasks that require long-term memory. Secondly it is robust to input noise and missing data because LSTMs are able to handle input sequences that have missing or corrupted data, making them resistant to noise. Long Short-Term Memory (LSTM) is widely used for continuous time series data prediction in various fields such as Traffic forecasting: LSTMs have been used to predict traffic flow [Tian & Pan, 2015], Energy demand forecasting: LSTMs have been used to predict energy demand [Torres, Martínez-Álvarez & Troncoso, 2022], and Weather forecasting: LSTMs have been used to predict various weather variables such as temperature and precipitation

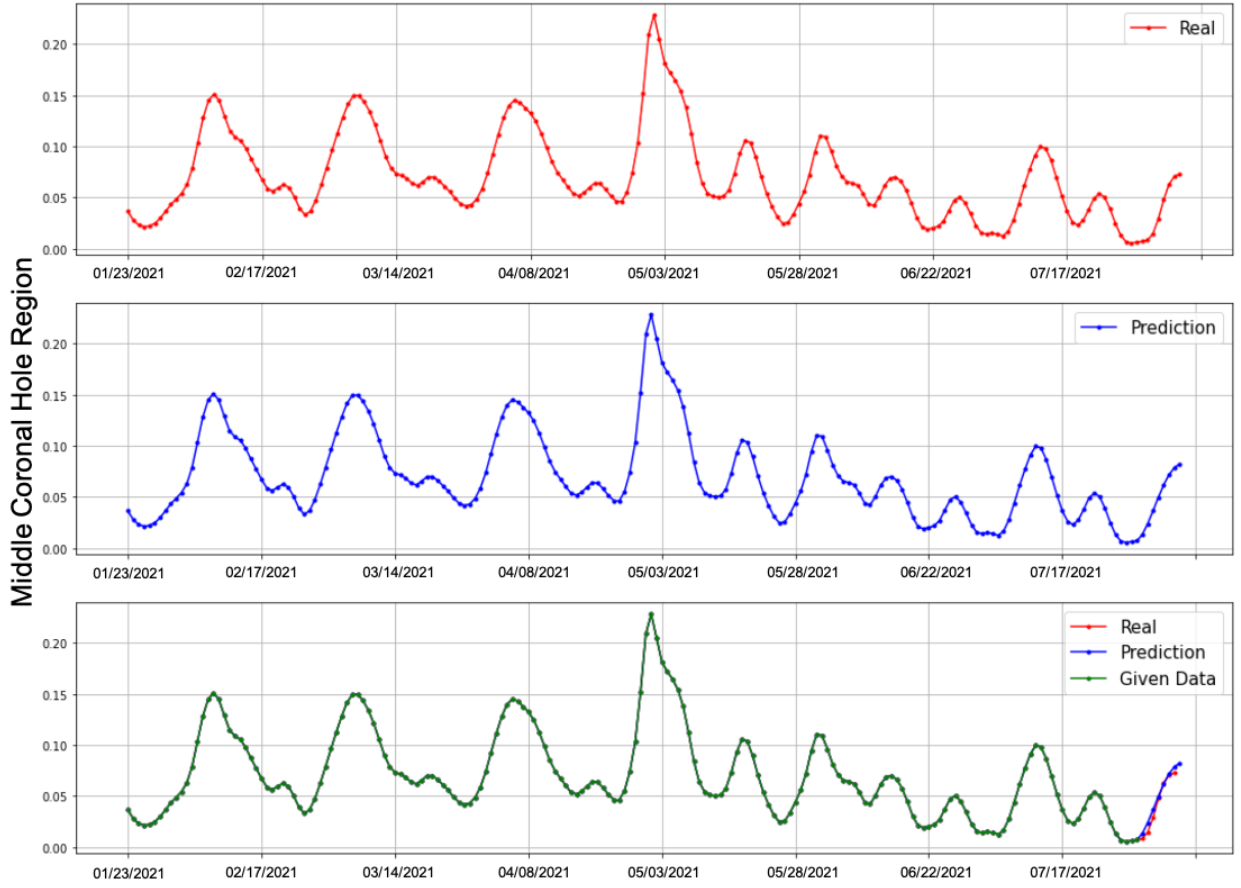


**Figure 13.** A comparison of actual middle area and predicted values for a 7-day period from July 31, 2021 to August 06, 2021, obtained after training the area data of 3847 middle coronal hole using LSTM from January 06, 2011 to July 30, 2021. The graph illustrates the accuracy of the LSTM model in predicting the area of the coronal hole in the middle region over a short-term period.

[Yang et al., 2019]. LSTM has proven to be efficient in capturing the temporal dependencies in time series data, which makes it well suited for forecasting tasks.

The goal of this study is to develop a model for predicting the area of coronal holes in a specific region on the Sun in the future. Coronal holes are areas of the solar corona that are characterized by low density and temperature, and they are closely linked to the solar wind, a stream of high-speed charged particles that can impact satellite and power grid operations on Earth. Thus, accurate prediction of the area of coronal holes is crucial for forecasting space weather events and mitigating their impacts on human activities. To achieve this goal, we used a Long Short-Term Memory (LSTM) technique, a type of deep learning model that is well-suited for time-series forecasting. LSTM models have the ability to capture long-term dependencies in the data, which is important for predicting the area of coronal holes, which can vary over the solar cycle, a period of about 11 years. In contrast, image-based models, such as Convolutional Neural Network (CNN) models, are not suitable for fast prediction because they require a lot of computational resources and time to train. We used 10 years of coronal hole area data to train the LSTM model and then used it to predict the area of the coronal hole in a specific region, the Middle area, in the future.

The results, shown in Fig. 12, indicate that the LSTM

model was able to accurately predict the area of the coronal hole using only 10 years of data. This suggests that the LSTM model was able to effectively capture the long-term dependencies present in the data, allowing it to make accurate predictions about the future. The use of LSTM models for time-series forecasting in space weather fields shows promising results. It is efficient in terms of computational speed and it is able to predict the coronal hole area using only numerical data, which is more efficient than using image data directly. Furthermore, the LSTM model was able to accurately predict the area of the coronal hole in the future which is not used in the training data, which is a great achievement. However, it is important to note that 10 years of data is relatively short, and more long-term data is needed to fully understand the dynamics of the corona hole and its relationship with the solar cycle.

### 3.4 Results

Fig. 13 illustrates the results of our analysis of the area of the coronal hole in the Middle region of the Sun over a period of 7 days using the LSTM model. The figure shows that the model was able to accurately predict the area of the coronal hole for a period of 7 days after being trained on 10 years of data. This suggests that the LSTM model was able to effectively capture the long-term dependencies present in the

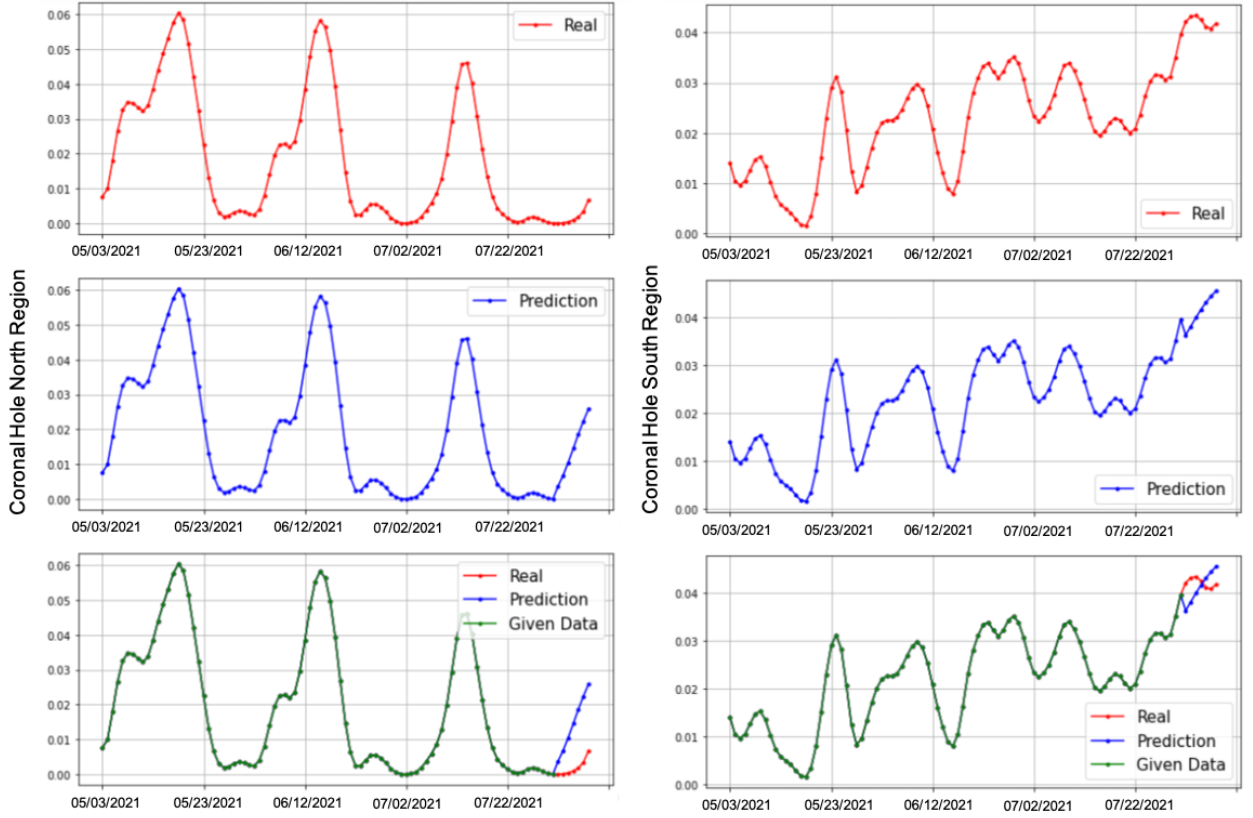


**Figure 14.** A comparison of actual pole area and predicted values for a 7-day period from July 31, 2021 to August 06, 2021, obtained after training the area data of 3847 pole coronal holes using LSTM from January 06, 2011 to July 30, 2021. The graph illustrates the accuracy of the LSTM model in predicting the area of the coronal hole in the pole regions over a short-term period.

data, allowing it to make accurate predictions about the future. The ability to predict the size of coronal holes has important implications for understanding and forecasting various phenomena caused by coronal holes, such as coronal mass ejections (CMEs) and corotating interaction regions (CIRs). CMEs are large eruptions of plasma and magnetic field from the solar corona, which can travel through interplanetary space and impact Earth's magnetosphere. CIRs are regions of high-speed solar wind streams that can produce geomagnetic storms and aurorae on Earth. By accurately forecasting the size and location of coronal holes, we may be able to better understand the mechanisms that drive CMEs and CIRs, and develop strategies for predicting and preparing for their impacts on Earth. Furthermore, Fig. 14 also demonstrates that the LSTM model was able to predict trends in the Arctic and Antarctic regions of the Sun, although not as accurate as in Middle area. Predicting the area of the coronal hole in the Arctic and Antarctic regions of the Sun could be important for understanding the impacts of space weather events on Earth. If it is found that coronal holes in these regions have an influence on Earth, it may be necessary to consider their size and location when forecasting geomagnetic activity and other space weather phenomena. In summary, this study highlights the potential of using deep learning techniques, such as LSTM models, for time-series forecasting in space weather fields. The LSTM model was able to accurately predict the area of the coronal hole in the future using only 10 years of data and it

could be a useful tool for predicting the size and location of coronal holes, which could help to enhance our understanding of space weather events and facilitate the development of strategies for predicting and preparing for their impacts on Earth. However, it is important to note that 10 years of data is relatively short, and more long-term data is needed to fully understand the dynamics of the corona hole and its relationship with the solar cycle.

## 4 Conclusions

### 4.1 Overall Summary

The development of an efficient and fast-operating coronal hole detection model has significant implications for space weather forecasting and the understanding of space weather phenomena. The coronal holes are regions in the solar corona characterized by low density and temperature, and they are closely linked to the solar wind, a stream of high-speed charged particles that can impact satellite and power grid operations on Earth. Therefore, the accurate prediction of the area of coronal holes is crucial for forecasting space weather events and mitigating their impacts on human activities.

In this study, we have developed a coronal hole detection model that allows us to extract a dataset of 3857 coronal hole data points. These data points were used to create a deep learning-based prediction model that can forecast

the size of coronal holes. This model represents a significant advancement in our ability to predict and understand space weather events, as it enables us to forecast changes in the coronal hole area. The use of deep learning techniques, such as LSTM models, for time-series forecasting in space weather fields shows promising results. It is efficient in terms of computational speed and it is able to predict the coronal hole area using only numerical data.

By using this model, we can better anticipate and prepare for space weather events that could impact Earth's space environment and technological systems, enhancing our ability to mitigate their effects. The ability to predict the size and location of coronal holes can help to improve our understanding of the mechanisms that drive CMEs and CIRs, and develop strategies for predicting and preparing for their impacts on Earth. Furthermore, it can also provide important information for mitigating the effects of space weather events on satellite and power grid operations. In conclusion, the development of this coronal hole detection and prediction model represents an important step forward in our understanding of space weather and its impacts on Earth. The model is efficient and able to predict the coronal hole area, which is essential for forecasting space weather events and mitigating their effects on human activities.

## 4.2 Limitation of Study

There are several limitations to this study that should be considered when interpreting the results. One limitation is that we are only predicting the area of the coronal hole, and not taking into account other space meteorological factors that may be influencing the size and location of the coronal hole. Space meteorology is a complex and interconnected system, and it is not yet fully understood how all of the various factors interact and influence each other. As a result, there may be additional factors that we are not considering that could impact the accuracy of our predictions.

Another limitation of this study is that we used a relatively short period of 10 years of data for the training and prediction of the coronal hole area. This period might not be long enough to capture the full variability of the coronal hole area and its relationship with the solar cycle. The solar cycle is an approximately 11-year period of variation in solar activity, including the number, size, and location of coronal holes, which can influence space weather events on Earth. Therefore, more long-term data is needed to fully understand the dynamics of the corona hole and its relationship with the solar cycle.

Additionally, this study only considered the coronal hole area in the Middle, Arctic and Antarctic regions, and not the whole solar surface. The coronal holes can also appear in other regions of the Sun, such as the equatorial region, which has the highest probability of producing CMEs and CIRs. Therefore, further research is needed to examine the coronal hole area in other regions and its relationship with space weather events.

Moreover, the study is based on a single instrument, AIA193 from NASA's Solar Dynamics Observatory (SDO). The use of additional data from other instruments and observatories could improve the accuracy of the coronal hole detection model and the predictions.

In conclusion, while this study has made significant progress in developing a coronal hole detection and prediction model, it is important to consider the limitations of the study when interpreting the results. The study only predicts the area of the coronal hole and does not take into account other space meteorological factors that may be influencing the size and location of the coronal hole. Additionally, it is based on a relatively short period of 10 years of data, which may not be long enough to capture the full variability of the coronal hole area.

## 4.3 Further Research

This study represents just the beginning of research on the prediction of coronal hole area and its potential impacts on space weather events. One potential direction for future research is to investigate the underlying physical processes that drive the formation and evolution of coronal holes. This could include studies of the Sun's magnetic field and its impact on the formation and location of coronal holes, as well as research into the mechanisms that drive the high-speed solar wind streams produced by coronal holes. By gaining a better understanding of these underlying processes, we may be able to improve our ability to predict the size and location of coronal holes, and more accurately forecast space weather events.

Additionally, there is also a need for the development of more sophisticated prediction models that can forecast the size and location of coronal holes over longer periods of time, such as the solar cycle. This will require the use of larger datasets and more advanced machine learning techniques.

Furthermore, it is also important to consider the potential impacts of coronal holes on other planets in our solar system, as they may be impacted by the solar wind streams produced by coronal holes. This could provide important insights into the impacts of space weather on other celestial bodies and help us to better understand the dynamics of space weather in our solar system.

This study represents an important step forward in understanding the dynamics of coronal holes and their relationship with space weather events. However, there is still much to learn about these phenomena and their impacts on Earth. By continuing to conduct research in this area, we can improve our ability to predict and prepare for space weather events, and better understand the complex space weather system that affects our planet.

## References

- Abramenko, V.I., Biktimirova, R.A. Magnetic Field of Coronal Holes During the Polarity Reversal. *Geomagn. Aeron.* 62, 869–872 (2022). <https://doi.org/10.1134/S0016793222070039>.
- Badruddin, A., and Falak, Z., (2016). Study of the geoeffectiveness of coronal mass ejections, corotating interaction regions and their associated structures observed during Solar Cycle 23. *Astrophys. Space Sci.* 361 (8), 253–316. <http://dx.doi.org/10.1007/s10509-016-2839-4>.

- Bartels, J., (1938). Potsdamer erdmagnetische Kennziffern, 1. Mitteilung. Zeitschrift für Geophysik, 14, 68–78. <https://doi.org/10.23689/fidgeo-3165>.
- Bartels, J., (1949). The standardized index, Ks, and the planetary index, Kp. IATME Bull., 12b, 97–120.
- Bengio, Y., (1994). Learning long-term dependencies with gradient descent is difficult. *IEEE Transactions on Neural Networks*, 5(2), 157-166. <http://dx.doi.org/10.1109/72.279181>.
- Bobrov, M. S., (1983), Non-recurrent geomagnetic disturbances from high-speed streams, *Planet. Space Sci.*, 31, 865.
- Boteler, David., (2013). Space Weather Effects on Power Systems. <http://dx.doi.org/10.1029/GM125p0347>.
- Buades, A., Coll, B., and Morel, J. M., (2005). A non-local algorithm for image denoising. In *2005 IEEE Computer Society Conference on Computer Vision and Pattern Recognition (CVPR'05)*, 2, 60-65. <http://dx.doi.org/10.1109/CVPR.2005.38>.
- Cranmer, S.R., (2009). Coronal Holes. *Living Rev. Sol. Phys.* 6, 3. <https://doi.org/10.12942/lrsp-2009-3>.
- Davis, K., (1990). Ionospheric Radio. Peter Peregrinus Ltd. London, UK.
- Eoin P. Carley, Nicole Vilmer, Angelos Vourlidas., (2020). Radio Observations of Coronal Mass Ejection Initiation and Development in the Low Solar Corona. *Frontiers in Astronomy and Space Sciences*, 7, 79. <https://doi.org/10.3389/fspas.2020.551558>.
- Filjar, R., (2001). Horizontal GPS Positioning Accuracy During the 1999 Solar Eclipse. *The Journal of Navigation*, 54:293–296. Cambridge University Press.
- Filjar, R., T. Kos., (2006). GPS Positioning Accuracy in Croatia during the Extreme Space Weather Conditions in September 2005. European Navigation Conference ENC 2006. Manchester, UK.
- Filjar, R., (2008). A Study Of Direct Severe Space Weather Effects On GPS Ionospheric Delay. *Journal of Navigation*, 61(1), 115-128. <http://dx.doi.org/10.1017/S0373463307004420>.
- Gonzalez, R. C., & Woods, R. E. (2006). *Digital image processing* (3rd ed.). Boston, MA: Pearson Education.
- B Heber, T.R Sanderson, M Zhang., (1999). Corotating interaction regions, *Advances in Space Research*, 23, 3, 567-579. [https://doi.org/10.1016/S0273-1177\(99\)80013-1](https://doi.org/10.1016/S0273-1177(99)80013-1).
- Heinemann, M., Barra, V., Neupert, W. M., & Koza, J., (2019). Detection of coronal holes from SDO/AIA EUV images. *Astronomy and Astrophysics*, 627, A78. <http://dx.doi.org/10.1051/0004-6361/201834235>.
- Sepp Hochreiter, Jürgen Schmidhuber., (1997). Long Short-Term Memory. *Neural Computation*, 9 (8): 1735–1780. <https://doi.org/10.1162/neco.1997.9.8.1735>.
- Inoue, S., (2016). Magnetohydrodynamics modeling of coronal magnetic field and solar eruptions based on the photospheric magnetic field. *Prog. in Earth and Planet. Sci.* 3, 19. <https://doi.org/10.1186/s40645-016-0084-7>.
- Jarolim, R., (2021). Multi-Channel Coronal Hole Detection with Convolutional Neural Networks. <https://doi.org/10.5194/egusphere-egu21-1490>.
- Kappenman, J. G., (1996). Geomagnetic storms and their impact on power systems. *IEEE Power Engineering Review*. 16, 5, 46-53. <https://doi.org/10.1109/MPER.1996.491910>
- Lemen, J.R., Title, A.M., Akin, D.J. et al., (2012) The Atmospheric Imaging Assembly (AIA) on the Solar Dynamics Observatory (SDO). *Sol Phys* 275, 17–40. <https://doi.org/10.1007/s11207-011-9776-8>
- Lipton, Z. C., Koc, K., & Bao, J. (2015). A critical review of recurrent neural networks for sequence learning. *arXiv preprint*
- Marr, D., (1980). Theory of edge detection. *Proceedings of the Royal Society of London B: Biological Sciences*, 207(1167), 187-217. <https://doi.org/10.1098/rspb.1980.0020>
- Matzka, J., Stolle, C., Yamazaki, Y., Bronkalla, O., & Morschhauser, A., (2021). The geomagnetic Kp index and derived indices of geomagnetic activity. *Space Weather*, 19, e2020SW002641. <https://doi.org/10.1029/2020SW002641>.
- McIntosh, P. S., Willock, E. C., and Thompson, R. J. (1991). Atlas of stackplots: 1966-1987. UAG-101," in World Data Center A for Solar-Terrestrial Physics (Boulder, CO: NOAA National Geophysical Data Center).
- Mursula, K., and B. Zeiger., (1996), The 13.5-day periodicity in the sun, solar wind, and geomagnetic activity: The last three solar cycles, *J. Geophys. Res.*, 101, 27,077. <https://doi.org/10.1029/96JA02470>.
- NASA. (n.d.). Solar Dynamics Observatory (SDO). Retrieved from <https://sdo.gsfc.nasa.gov/>.
- National Oceanic and Atmospheric Administration. (n.d.). Space weather. Retrieved from <https://www.noaa.gov/education/resource-collections/space-weather>.
- NOAA. (2021). AP index. Retrieved from <https://www.swpc.noaa.gov/products/geospace-indices>.
- Pascanu, R., Mikolov, T., & Bengio, Y. (2013). On the difficulty of training recurrent neural networks. *International Conference on Machine Learning*, 1310-1318.

- Rama Rao, P. V. S., Gopi Krishna, S., Vara Prasad, J., Prasad, S. N. V. S., Prasad, D. S. V. V. D., and Niranjan, K., (2009). Geomagnetic storm effects on GPS based navigation, *Ann. Geophys.*, 27, 2101–2110, <https://doi.org/10.5194/angeo-27-2101-2009>.
- Richardson, I. G., E. W. Cliver, and H. V. Cane., (2000), Sources of magnetic activity over the solar cycle: Relative importance of coronal mass ejections, high-speed streams, and slow solar wind, *J. Geophys. Res.*, 105, 18, 203.
- Richardson, I. G., E. W. Cliver, and H. V. Cane., (2001), Sources of geomagnetic storms for solar minimum and maximum conditions during 1972–2000, *Geophys. Res. Lett.*, 28, 2569.
- Sandford, W. H., (1999). The Impact on Solar Winds on Navigation Aids. *The Journal. of Navigation*, 52, 42–46.
- Schwenn, R., (2006) Space Weather: The Solar Perspective. *Living Rev. Sol. Phys.* 3, 2. <https://doi.org/10.12942/lrsp-2006-2>.
- Y. Tian and L. Pan., (2015). Predicting Short-Term Traffic Flow by Long Short-Term Memory Recurrent Neural Network. *IEEE International Conference on Smart City*, 153-158. <https://doi.org/10.1109/SmartCity.2015.63>.
- Torres, J.F., Martínez-Álvarez, F. & Troncoso., (2022). A deep LSTM network for the Spanish electricity consumption forecasting. *Neural Comput & Applic*, 34, 10533–10545. <https://doi.org/10.1007/s00521-021-06773-2>.
- Webb, D.F., Howard, T.A., (2012). Coronal Mass Ejections: Observations. *Living Rev. Sol. Phys.* 9, 3. <https://doi.org/10.12942/lrsp-2012-3>.
- Yang, B., Sun, S., Li, J., Lin, X., & Tian, Y. (2019). Traffic flow prediction using LSTM with feature enhancement. *Neurocomputing*, 332, 320-327. <https://doi.org/10.1016/j.neucom.2018.12.016>
- Yashiro, S., N. Gopalswamy, G. Michalek, O. C. St. Cyr, S. P. Plunkett, N. B. Rich, and R. A. Howard., (2004). A catalog of white light coronal mass ejections observed by the SOHO spacecraft, *J. Geophys. Res.*, 109, A07105, <https://doi.org/10.1029/2003JA010282>.